ACTA ASTRONOMICA
Vol. **61** (2011) pp. 123–138

The Optical Gravitational Lensing Experiment. Dwarf Novae in the OGLE Data. I. Three New Dwarf Novae: One in the Period Gap and Two Longer Period Objects*

R. Poleski[1], A. Udalski[1], J. Skowron[2], M.K. Szymański[1], M. Kubiak[1], G. Pietrzyński[1,3], I. Soszyński[1], S. Kozłowski[1], P. Pietrukowicz[1], Ł. Wyrzykowski[1,4] and K. Ulaczyk[1]

[1] Warsaw University Observatory, Al. Ujazdowskie 4, 00-478 Warszawa, Poland
e-mail: (rpoleski,udalski,msz,mk,pietrzyn,soszynsk,simkoz,pietruk,wyrzykow,kulaczyk)@astrouw.edu.pl
[2] Department of Astronomy, Ohio State University, 140 W. 18th Ave., Columbus, OH 43210, USA
e-mail: jskowron@astronomy.ohio-state.edu
[3] Universidad de Concepción, Departamento de Astronomia, Casilla 160-C, Concepción, Chile
[4] Institute of Astronomy, University of Cambridge, Madingley Road, Cambridge CB3 0HA, UK

Received June 29, 2011

ABSTRACT

We report serendipitous discovery of three new dwarf novae which eruptions in 2010 were observed by the ongoing microlensing survey OGLE-IV. All three objects are located in the Galactic bulge fields observed with the highest cadence of 20 minutes. In the OGLE-III and OGLE-IV data we revealed a total of 23 outbursts for one of the stars. What makes this object most interesting is the derived superhump period of 2.61 h placing it in the orbital period gap. The superhump period changed during the superoutburst with a very short timescale. For two other objects, for which we observed outburst, the orbital periods of 5.4 h and 9.5 h were measured in the quiescence.

Key words: *novae, cataclysmic variables – binaries: close – surveys*

1. Introduction

Because outbursts of dwarf novae (DNe) are unpredictable astrophysical phenomena, discovering new objects of this class has been, for the very long time,

*Based on observations obtained with the 1.3 m Warsaw telescope at the Las Campanas Observatory of the Carnegie Institution for Science.

domain of amateur astronomers. The situation has changed in the last couple of years when massive sky surveys started regular monitoring of large areas of the sky or the densest stellar regions in the sky. Tens new cataclysmic variables (CVs) were detected by the SDSS sky survey (*e.g.*, Szkody *et al.* 2007, Southworth *et al.* 2010) or microlensing surveys (Cieslinski *et al.* 2003, 2004).

The OGLE (Optical Gravitational Lensing Experiment) microlensing survey is regularly monitoring millions of stars for microlensing events toward the Galactic center and Magellanic Clouds since early 1990s. It regularly detected many outbursts of DNe in the observed fields. The algorithm of real time detection system of microlensing events – EWS system (Udalski 2003) – in the natural way detected also brightenings of outbursting DNe (Skowron *et al.* 2009). However, these objects were usually treated as the background noise in the microlensing detection process and then neglected. The only study of CVs based on the limited OGLE-II data was done by Cieslinski *et al.* (2003).

The OGLE microlensing data collected during the first three phases of the project OGLE-I – OGLE-III (1992–2009) while providing very precise long term photometry have only limited applications in the characterization of DNe. They could be used for the detection of new DNe, constraining their frequency of occurrence or analysis of frequency of outbursts. However, the typical cadence of observations in these phases, namely one/two observations per night, prevented more accurate characterization of outbursts lasting typically a few days. On the other hand the OGLE data are well suited and were successfully used for characterization of slower variability CVs like, for example, Nova Sco 2008 – V1309 Sco (Tylenda *et al.* 2011).

New generation phase of the OGLE survey, OGLE-IV, that started in March 2010, provides new observing capabilities that completely change the above limitations. Several 1.4 square degrees fields in the direction of the Galactic bulge are now regularly observed with the cadence of 20 or 60 minutes. This enables studies of all ultra-short time variable objects including the outbursts of even so short periodic variables as from the SU UMa type subgroup of DNe.

Here, in this pilot paper, we present three examples of OGLE-IV observations of outbursts of DNe to show the potential and capabilities of the new OGLE-IV survey. Encouraged by these early results we decided to carry out more comprehensive search for CVs in the already collected OGLE-IV data as well as to save all the CVs detected in real time by the OGLE-IV EWS microlensing system and then analyze properties of the detected objects. Results will be presented in the subsequent papers of this series.

Dwarf novae are semidetached binary systems with Roche lobe filling main sequence secondary which matter is accreted *via* a disk onto the white dwarf primary. The most easily noticeable features in the distribution of known DNe orbital periods (Knigge 2006) are the presence of a sharp period minimum (76 minutes) and the period gap between 2 and 3 hours where the number of systems found is

very low. In objects with periods longer than the upper limit of the period gap the accretion is driven by the angular momentum loss of the secondary by magnetic braking. This process stops when the secondary becomes fully convective which is predicted at an orbital period of $P_{\rm orb} = 2.85$ h by models of Howell *et al.* (2001). The boundary value derived from the histogram of observed systems by Knigge (2006) is 3.18 h with smaller discontinuity seen close to the value of Howell *et al.* (2001). At this stage the mass transfer ceases and the secondary star reestablishes the Roche lobe contact, when the period drops to 2.15 h (Howell *et al.* 2001, or 2.10 h as found by Knigge 2006). Further evolution of the system is governed by the angular momentum loss driven by the emission of gravitational waves.

The periodic brightness changes observed in the quiescence may be caused by changing visibility of the hot spot (hot part of the disk where a stream of matter reaches the disk). In systems with $P_{\rm orb} > 5$ h the secondary contributes significant flux to the total flux of the system (Warner 2003) and the double wave ellipsoidal variations caused by the distorted secondary can be seen, if the inclination of the system is high enough. The stars presented in this paper are located in the dense stellar region and the possibility of blending with other, possibly variable, sources can not be ruled out. Blending also lowers the amplitude of the outbursts.

During the superoubursts we expect to see superhumps which manifest as a tooth-shaped light variations with an amplitude of up to 0.5 mag (*e.g.*, Semeniuk *et al.* 1997). The superhump period, which may be changing, is typically a few percent longer than the orbital period. This period excess is greater for systems with longer orbital periods (Stolz and Schoembs 1984).

In the Section 2 we give an overview of photometric data used. The three following sections describe new DNe. We end with a summary and future plans.

2. Observations

The main dataset analyzed in this work comes from the OGLE-IV survey which started in March 2010. This ongoing survey uses 1.3-m Warsaw telescope located at Las Campanas Observatory, Chile. The observatory is operated by the Carnegie Institution for Science. The mosaic camera consists of 32 CCD chips 2048×4102 pixels each. The total field of view is 1.4 square degrees. Pixel size of 15μm corresponds to $0\farcs26$ in the sky. Most of the observations are taken with the *I*-band filter with an exposure time of 100 s. Data of some objects acquired between Julian days 2 455 250 and 2 455 375 may be affected by technical problem which manifests itself through a higher scatter of the data or shifted mean brightness. The main goal of the OGLE-IV survey is to observe central Galactic bulge fields frequently enough to see planetary perturbations in the gravitational microlensing events in regular survey mode *i.e.*, without finding them while ongoing and intensifying the observations. Three fields named BLG501, BLG504 and BLG505 with equatorial coordinates of the centers $(\alpha, \delta) = (17{:}51{:}53, -29{:}50{:}45)$, $(17{:}57{:}30, -28{:}00{:}00)$

and $(17{:}57{:}30, -29{:}13{:}50)$, respectively, are observed with a cadence of 20 minutes[†]. This provides a unique opportunity to study other transient phenomena like the dwarf novae eruptions with high time resolution.

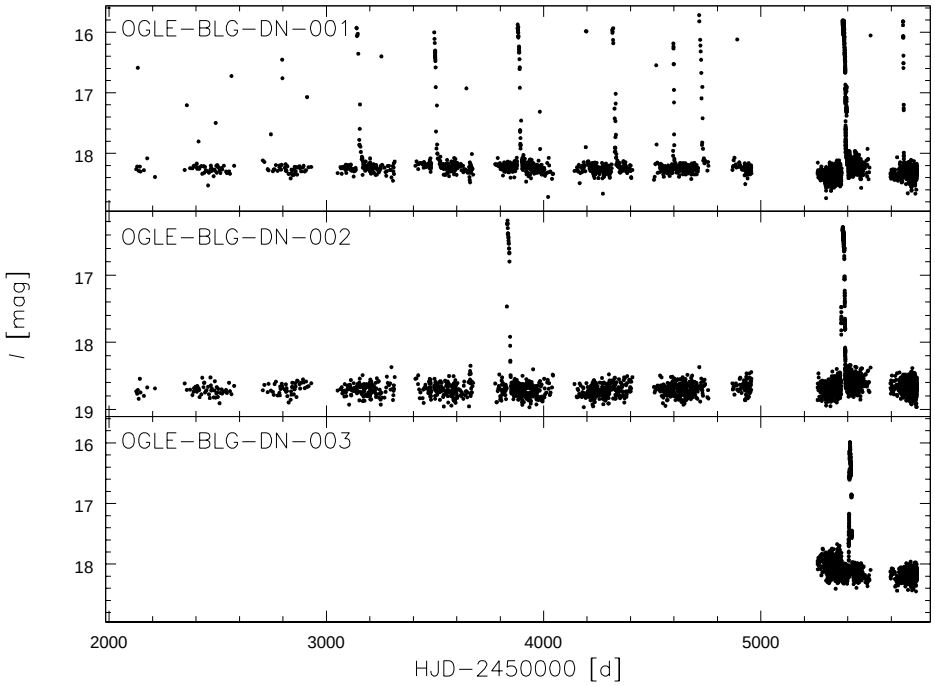

Fig. 1. OGLE-III and OGLE-IV light curves for the analyzed DNe.

Central parts of the Galactic bulge were also observed in the previous phases of the OGLE survey. During the third phase (OGLE-III) the same telescope was used with the camera containing eight CCD chips. Observations lasted from 2001 to 2009. Details of the setup and data reduction were given elsewhere (Udalski 2003, Udalski *et al.* 2008). The colors of the dwarf novae change in the *a priori* unknown way, thus we did not apply corrections to instrumental magnitudes described by Udalski *et al.* (2008), which may change the zero point of magnitude scale by 0.1 mag.

The photometry was obtained using the Difference Image Analysis (DIA) method (Alard and Lupton 1998, Alard 2000, Woźniak 2000). We supplemented the OGLE-IV photometric data with the OGLE-III ones, if available. Whole analyzed dataset is presented in Fig. 1.

Table 1 gives basic parameters of analyzed stars together with the number of measurements during the third and the fourth phase of the OGLE survey. We have checked centroids from the OGLE-III PSF photometry (OGLE-BLG-DN-001 and

[†]See the OGLE webpage *http://ogle.astrouw.edu.pl* for the sky coverage and the cadence of other fields.

T a b l e 1

Basic data of analyzed stars

ID	RA	Dec	I_q [mag]	$I_{\max}$ [mag]	N_{O3}	N_{O4}
OGLE-BLG-DN-001	$17^h53^m10\overset{s}{.}04$	$-29^\circ21'20\overset{''}{.}6$	$18.62-17.96^a$	15.72	1354	2487
OGLE-BLG-DN-002	$17^h53^m18\overset{s}{.}69$	$-29^\circ17'17\overset{''}{.}3$	$18.97-18.34^a$	16.18	1354	2472
OGLE-BLG-DN-003	$17^h56^m07\overset{s}{.}27$	$-27^\circ48'47\overset{''}{.}5$	$18.45-17.96$	15.99	0	2461

I_q is brightness range in quiescence (^{a} – blended with other object), $I_{\max}$ is maximum recorded brightness, N_{O3} and N_{O4} are the numbers of measurements in the OGLE-III and the OGLE-IV data, respectively.

OGLE-BLG-DN-002) and DIA centroids from OGLE-IV (OGLE-BLG-DN-003). For OGLE-BLG-DN-001 and OGLE-BLG-DN-002 we have clearly found shift between apparent centroid of the stars in the quiescence and close to the maximum brightness. This shows that the two objects are blended and they are fainter than the brightness in the quiescence (I_q) given in Table 1. Finding charts are presented in Fig. 2.

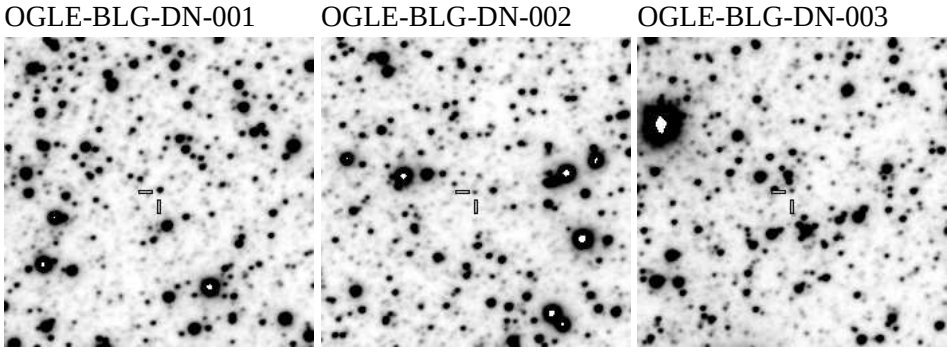

Fig. 2. Finding charts of analyzed stars. North is up, East is to the left. These subframes of *I*-band images cover $60'' \times 60''$.

3. OGLE-BLG-DN-001

The whole OGLE light curve of this object is shown in the upper panel of Fig. 1. For most outbursts we have only one or two observations, thus, to ensure these are not some kind of an artifacts of the DIA photometry, we have carefully checked PSF photometry for OGLE-III data (Udalski *et al.* 2008) and examined the last image of the field taken in 2010 season of OGLE-IV. In all cases we confirmed that the object was in the bright state and each point brighter than 17.9 mag belongs to one of the outbursts.

3.1. Outbursts: Shapes and Frequencies

Results of timing of outbursts are given in Table 2 which gives $\mathrm{HJD}'_{\mathrm{max}}$ (hereafter $\mathrm{HJD}' \equiv \mathrm{HJD} - 2\,450\,000$) and maximum recorded brightness I_{max} if it was brighter than 16.5 mag. In total 23 events were observed. The time interval between definite superoutbursts is between 354 and 435 days with an exception of 662 d, when a gap between the OGLE-III and the OGLE-IV occurs. It is possible that the supercycle is two times shorter and superoutbursts occurred during the seasonal gaps. In that case the ratio of supercycle length to normal cycle length would be small compared to other SU UMa type stars (Warner 2003). We suppose that also observations done at $\mathrm{HJD}' = 2358$ and 2745 caught the superoutbursts rather than the normal outbursts. Firstly because the time difference between them is 387 d and the next superoutburst occurs 392 d later, which fits well to the time intervals of the superoutbursts given above, and secondly, a few days before and after these observations were done no other observation was secured. Fig. 3 shows the

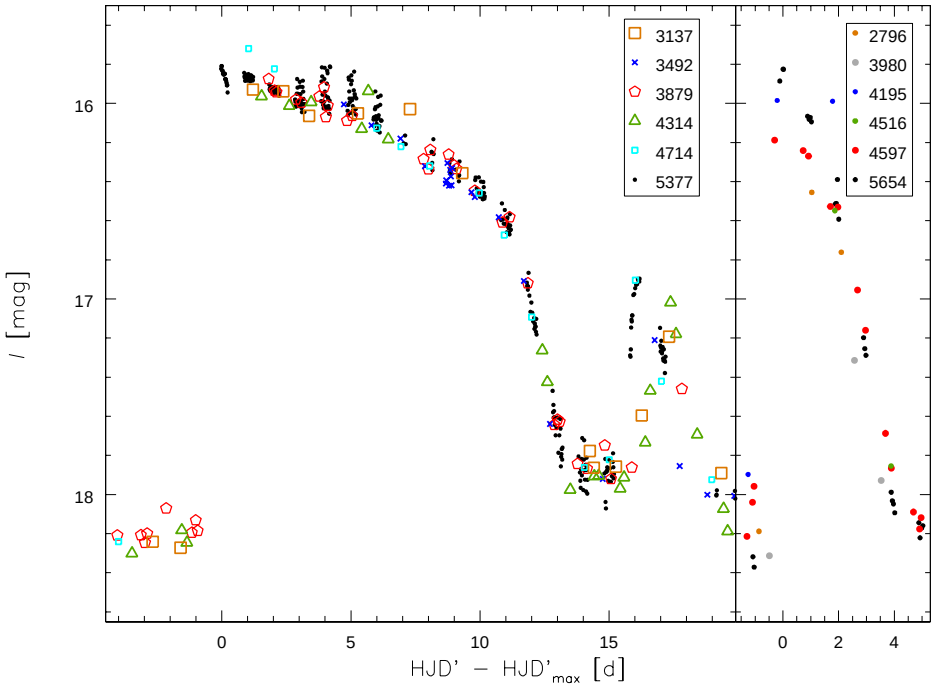

Fig. 3. Aligned profiles of the superoutbursts (*left panel*) and the normal outbursts (*right panel*) of OGLE-BLG-DN-001. Different outbursts are indicated by different symbols and labeled. Zero on the horizontal axis corresponds to the time of maximum light.

profiles of the superoutbursts (left panel) and the normal outburst (right panel). All events with more than one observation were shifted to fit the plateau phase and final decline. The $\mathrm{HJD}' = 2358$ observation fits a superoutburst profile, if it was done during the brightening of the object before the plateau and the next observation was

done just after the superoutburst ended. The $\mathrm{HJD}' = 2745$ observation had to be obtained while the object was fading after the plateau. The point at 11 days earlier was taken just before the superoutburst started and the whole event was slightly shorter than the ones shown on the left panel of Fig. 3.

T a b l e 2

Outburst timing of OGLE-BLG-DN-001

$\mathrm{HJD}'_{\mathrm{max}}$	I_{max} [mag]	comments
2133		1 point
2358		1 point, probable superoutburst[a]
2411		1 point
2491		1 point
2563		1 point
2745		1 point, probable superoutburst[a]
2796	16.46	2 points
2911		1 point
3137	15.93	superoutburst with echo and probable superhumps[a]
3253	16.40	1 point
3492	16.00	superoutburst with echo
3644		1 point
3879	15.87	superoutburst with echo
3980		2 points
4195	15.98	2 points
4314	15.96	superoutburst with echo and probable superhumps[a]
4516		2 points
4597	16.19	
4714	15.72	superoutburst with echo
4891	16.12	1 point
5377	15.81	superoutburst with echo and superhumps
5504	16.06	1 point
5654	15.82	

[a] – see text for details

The estimation of the time interval between the normal outbursts is more complicated than for the superoutbursts. We might have missed a few of them because of a few days long gaps in the OGLE-III data and seasonal breaks when the Galactic bulge was not observed. The best estimate of a typical time interval is around 80 days but a better constraint can be given when a few years long coverage by the OGLE-IV data with at least one measurement per night will be available.

The left panel of Fig. 3 shows that we have never caught the object during its brightening to the maximum light of the superoutburst. The shortest time difference between the last point in quiescence and the first point in superoutburst is 2.98 d for $\mathrm{HJD}' = 3879$ superoutburst. Typically object fades by 0.07 mag per day during the plateau phase. The length of the superoutburst is around 12 days. Each definite superoutburst of the OGLE-BLG-DN-001 is showing an echo outburst with an

amplitude two times smaller than the normal outbursts. These echo outbursts may have two distinct profiles one for superoutbursts 3137 and 4314 with all the other belonging to the second group. Osaki *et al.* (2001) suggested such echo outbursts may be caused by changes of viscosity in the cold disk.

The amplitudes of normal outbursts are similar to the ones of the superoutbursts, which is atypical for the SU UMa type stars. For most stars of this type the superoutbursts are brighter by 0.7 mag (Warner 2003). For OGLE-BLG-DN-001 the normal outbursts are three times shorter than the superoutbursts.

3.2. Superhumps

The $\mathrm{HJD}' = 5377$ superoutburst was observed with a cadence of around 20 minutes. It allows more detail analysis of this event. Fig. 4 presents the plateau phase with model fitted in the upper panel. The superhumps are clearly seen between $\mathrm{HJD}' = 5379$ and 5383. These data together with those from the previous night, when most likely the superhumps started, are shown in panel *b* of Fig. 4 after the fit was subtracted. The second part of the plateau has much worse coverage and cannot give any firm conclusions about the existence of the superhumps. Panel *c* of Fig. 4 shows the evolution of superhump amplitude. It reaches maximum value a few days after supermaximum and then slowly decreases.

We determined the times of superhump maximum light and fitted the linear ephemeris to them:

$$\mathrm{HJD}' = 5379.5826(45) + 0.10412(25) \cdot E.$$

Last panel of Fig. 4 shows the $O-C$ diagram for the derived times of maximum light (Table 3). The fitted parabola corresponds to the superhump period P_{sh} changing according to the formula:

$$P_{\mathrm{sh}} = 0.10680(67) - 0.00165(50) \cdot (\mathrm{HJD}' - 5379). \quad (1)$$

A separate analysis of the superhump data was performed using the multiharmonic analysis of variance (MHAOV) method (Schwarzenberg-Czerny 1996). Periods were derived for data from each night and the linear regression resulted in the following ephemeris:

$$P_{\mathrm{sh}} = 0.10990(52) - 0.00256(22) \cdot (\mathrm{HJD}' - 5379). \quad (2)$$

Results from Eqs. (1) and (2) altogether give the best estimate of P_{sh} at the beginning of the superhumps ($\mathrm{HJD}' \approx 5379$) equal to $0.1087\ \mathrm{d} = 2.61\ \mathrm{h}$. Even though we have not measured the orbital period directly, we suggest this object lies inside the period gap. We used the dependence of the period excess $\varepsilon = (P_{\mathrm{orb}} - P_{\mathrm{sh}})/P_{\mathrm{orb}}$ on P_{orb} (Olech *et al.* 2011), to draw upper and lower envelope relations and from these relations we found P_{orb} should be between 0.098 and 0.101 d (2.35 and 2.42 h, respectively). We note that the period excess should be at least

T a b l e 3

Superhump maxima of OGLE-BLG-DN-001

E	HJD'	E	HJD'
0	5379.5704	19	5381.5646
1	5379.6732	20	5381.6720
2	5379.7884	21	5381.7767
9	5380.5259	29	5382.5953
10	5380.6324	30	5382.7006
11	5380.7374	31	5382.7991
12	5380.8405		

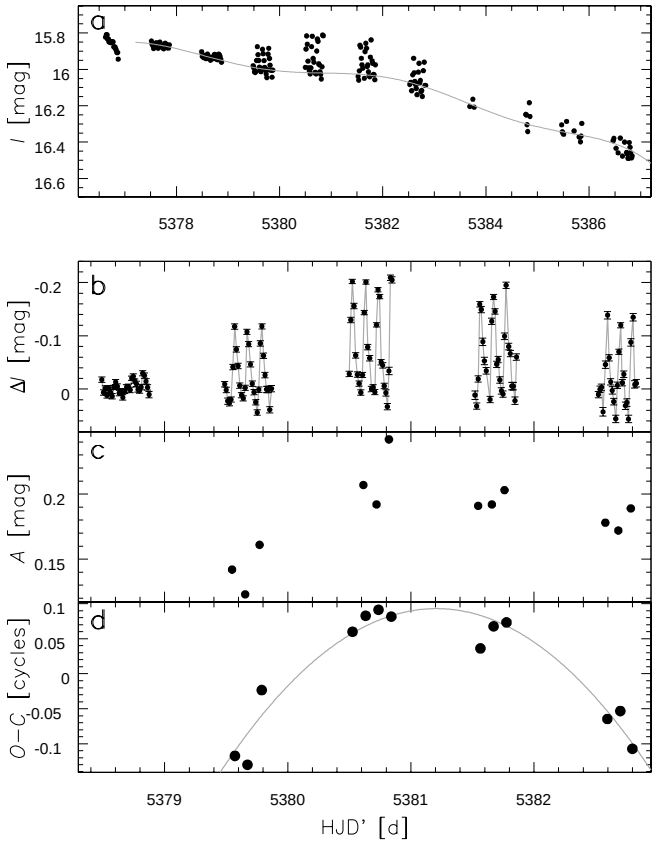

Fig. 4. Light curve of OGLE-BLG-DN-001 plateau phase (*upper panel*) with model fitted to data without superhumps. *Lower panels* show a closeup of the superhump data (consecutive points are connected for clarity), superhumps amplitude *vs.* time and $O-C$ diagram for superhumps maxima, respectively.

21%, if the orbital period is at the edge of the period gap (2.15 h). This value of the period excess is not expected for a CV (Olech *et al.* 2011).

The time derivative of $P_{\rm sh}$ is $-2\cdot10^{-3}$. Two different methods were used to estimate this value and their results are not the same. That is because the $O-C$ method uses only brightness maxima and is sensitive to the changes in their shape, phase etc. The MHAOV method uses whole light curve. Similarly large negative values of the time derivative of $P_{\rm sh}$ were found only in MN Dra, NY Ser and SDSS J162520.29+120308.7 (Kato *et al.* 2009, Olech *et al.* 2011). All these objects are situated inside the period gap.

We note that there are two observations taken at HJD$'\approx3882.8$ with a time difference of 0.0742 d (*i.e.*, 0.71 of $P_{\rm sh}$) and brightness difference of 0.15 mag. Similarly there are two observations taken at HJD$'\approx4319.6$ with the differences of 0.2548 d (*i.e.*, 2.4 of $P_{\rm sh}$) and 0.19 mag, respectively. We do not expect such brightness changes to be caused by the decline during the plateau and suggest that also HJD$'=3879$ and 4314 superoutbursts were showing superhumps.

Using MHAOV analysis we tried to search for other periodicities both after prewhitening plateau data, in quiescence and after subtracting the echo outburst profile. No sign of a periodic light variations was found.

4. OGLE-BLG-DN-002

This object was announced by the MOA group (Sako *et al.* 2008) as a candidate microlensing event with designation MOA-2010-BLG-338. The whole light curve is shown in the middle panel of Fig. 1 and the close-up of two outbursts observed by the OGLE-III and the OGLE-IV are shown in Fig. 5. They are 1543 days apart and, if the same time elapsed after the previous outburst, it should have taken place during the observing gap between the first two observing seasons of OGLE-III. Both outbursts show a plateau with brightness declining 0.05 mag per day and the shape characteristic for superoutbursts. The length of the second outburst is 2 d longer than the first one. We suspect that the second outburst might have been triggered by a precursor. During that time the observations were not conducted because of the final engineering of the OGLE-IV camera.

The plateau data (HJD$'$ in the range 5376–5383) were analyzed to search for a possible superhumps. For each night the trend was subtracted and the MHAOV periodogram with two harmonics was calculated. It is shown in Fig. 6 together with data folded with the period of $P_1=0.22431(66)$ d corresponding to the highest peak in the power spectrum. The second highest peak corresponds to the period two times longer. The profile of the brightness changes is more a tooth-like than a wave-like and is variable. Contrary to OGLE-BLG-DN-001, for OGLE-BLG-DN-002 it is not clear that the observed light variations were caused by the superhumps. If we observed the superhumps, then such profiles are more characteristic for the late part of the plateau (*e.g.*, Semeniuk *et al.* 1997). The length of the P_1 does

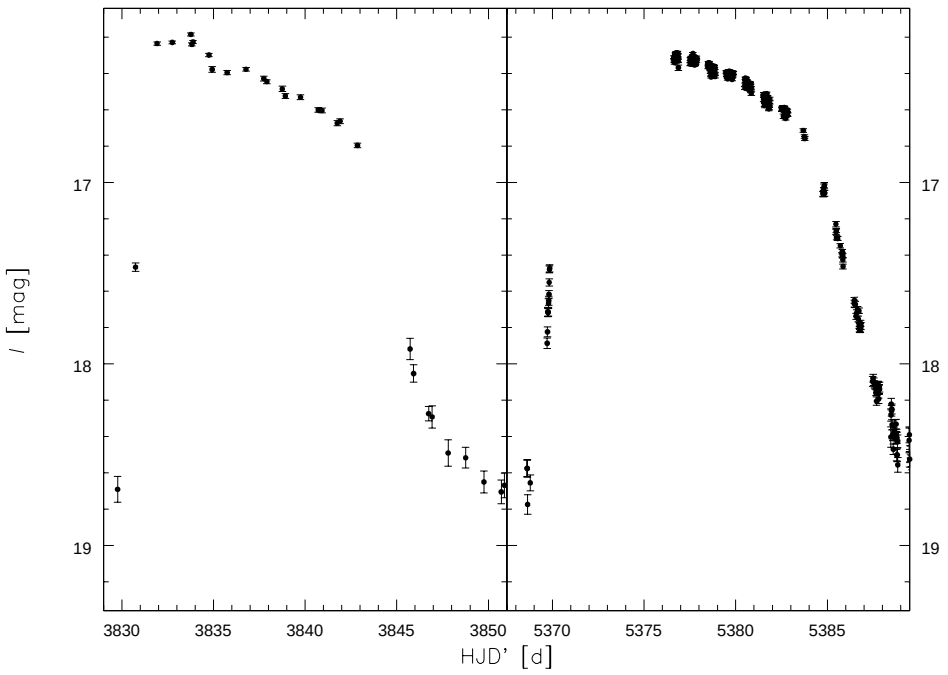

Fig. 5. Outbursts light curve of OGLE-BLG-DN-002 in the OGLE-III (*left*) and the OGLE-IV (*right*). The time span in both panels is the same.

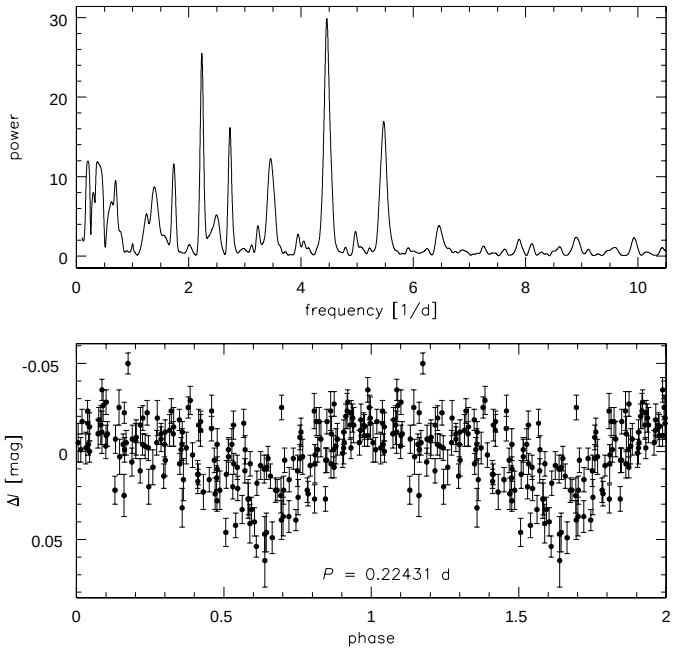

Fig. 6. Power spectrum of OGLE-BLG-DN-002 plateau data (*upper panel*) and these data phased with the period 0.22431 d corresponding to the highest peak in the power spectrum (*lower panel*).

not negate superhump hypothesis. Even though superhump periods are typically shorter than P_1, Retter *et al.* (2003) found superhumps with even longer period in TV Col which is an intermediate polar (see Warner 2003 for a review). Our analysis of OGLE-BLG-DN-002 is hampered by a small amplitude of the observed light variations, which is around 0.08 mag. Reliable determination of times of maximum light is not possible.

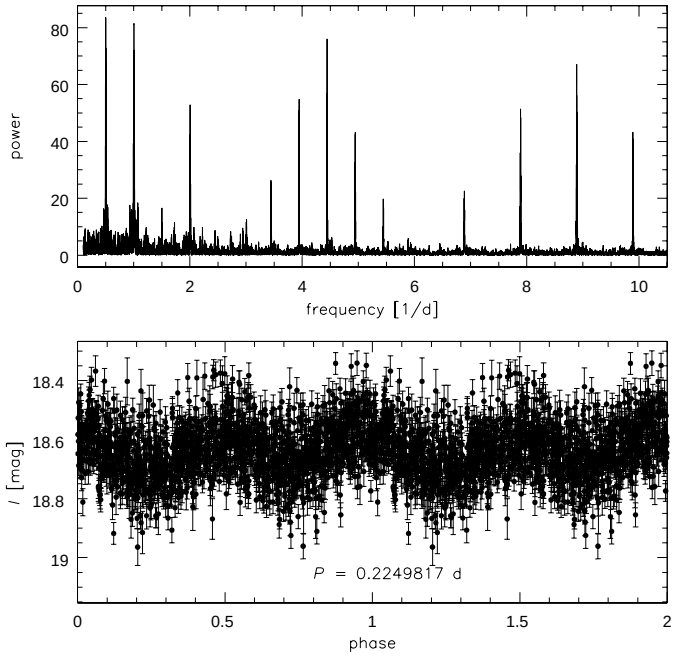

Fig. 7. Power spectrum of OGLE-BLG-DN-002 quiescence data (*upper panel*) and these data phased with period 0.2249817 d corresponding to the peak near 4.4 1/d (*lower panel*).

We have also performed period analysis of the OGLE-IV quiescence data. The upper panel of Fig. 7 shows the MHAOV periodogram calculated with two harmonics. The two highest peaks in the periodogram correspond to ≈ 1 d and ≈ 2 d and they are caused by the observing pattern. The other peaks are near 4.44 1/d and 8.88 1/d. Also their one and two day aliases are clearly seen. The lower panel shows data phased with the period $P_2 = 0.2249817(35)$ d ($1/P_2 \approx 4.44$ 1/d). A small evidence for an asymmetry can be seen. The peak near 8.88 1/d corresponds to the quadruple wave which is very unlikely to be observed.

The period P_2 should be equal either $P_{\rm orb}$ or $2P_{\rm orb}$. During the plateau phase of the superoutburst, we have measured less precisely variations with a period P_1 which is indistinguishable from P_2 within uncertainties. The shape of the light curve suggests variations with P_1 may be superhumps. Thus, we interpret P_2 as being equal to the $P_{\rm orb}$ and P_1, which is less accurately known because of smaller number of measurements, to be $P_{\rm sh}$.

We prewhitend quiescence and plateau data with periods found and searched for other periodic variations. Nothing was found.

5. OGLE-BLG-DN-003

This object was announced by the MOA group as a candidate microlensing event and designated MOA-2010-BLG-466. Its field was not observed by the OGLE-III, thus we have only the OGLE-IV data which are shown in the bottom panel of Fig. 1. Only one outburst was observed and it is shown in detail in Fig. 8. The upper panel shows the whole outburst and smaller panels show data from the separate nights. The rising branch lasts longer than the plateau phase. It is not obvious, if this is a super- or a normal outburst.

To search for periodic light changes we subtracted a linear trend from each night between $\mathrm{HJD}' = 5405$ and 5419 separately. The first night of the outburst was omitted as it shows very large variations, which may be a superposition of the changes seen in the quiescence (see below) and possible superhumps. The MHAOV periodograms calculated with one and two harmonics, as well as data phased with two candidate periods ($P_3 = 0.19895(35)$ d and $P_4 = 0.39803(80)$ d) are shown in Fig. 9. The profiles of folded light curves do not resemble typical superhump ones.

To show brightness variations in the quiescence, we choose 42 days from 2011 season, during which 615 epochs were collected. Our findings are applicable to the other part of the quiescence but other light variations mask them if longer time span of observations is analyzed at once. The MHAOV periodogram calculated with two harmonics is shown in the upper panel of Fig. 10. Very high power was found with a main peak corresponding to period $P_5 = 0.397456(41)$ d. The analyzed part of the light curve folded with P_5 is shown in the bottom panel. It is clearly asymmetric double wave. We interpret P_5 as an orbital period. It is much longer than the upper limit of the period gap. Taking into account the odd shape of the outburst we suspect OGLE-BLG-DN-003 is atypical dwarf nova or possibly an intermediate polar. We note that the nightly brightness variations seen in Fig. 8 have amplitude that is consistent with the quiescence variations dumped by the increasing flux.

6. Summary and Future Plans

We present three new DNe found serendipitously in OGLE data. The most interesting results were found for OGLE-BLG-DN-001. This SU UMa subtype DN shows superoutbursts each ≈ 400 d and normal outbursts with a recurrence time of around 80 d. The measured P_{sh}, when superhumps emerge, is 2.61 h what is a very strong suggestion that the orbital period of this object is inside the period gap. The superhump period change rate is $-2 \cdot 10^{-3}$ what is a very large negative value for a DN, however similar to the ones found in other in-the-gap SU UMa type stars.

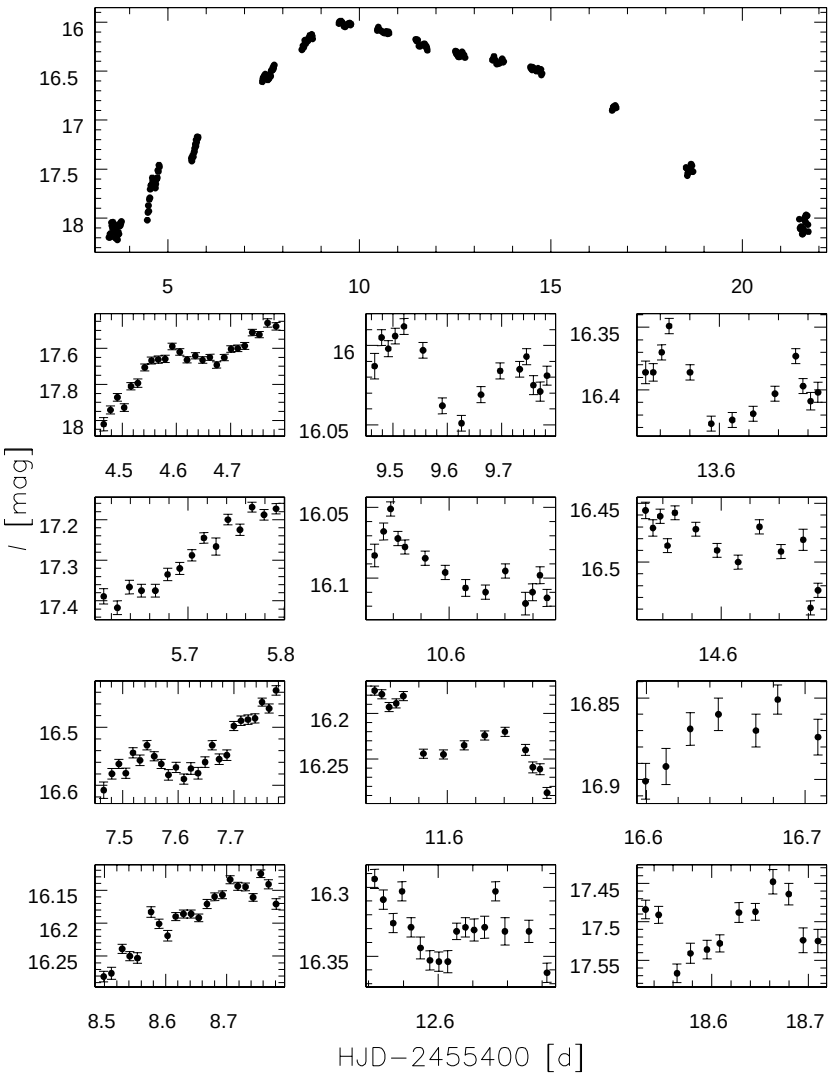

Fig. 8. Outburst light curve of OGLE-BLG-DN-003. *Smaller panels* show each outbursts night separately.

The orbital periods for OGLE-BLG-DN-002 and OGLE-BLG-DN-003 are most likely 5.40 h and 9.54 h, respectively. These values are well above the upper boundary of the orbital period gap. According to 7.15 version of the Ritter and Kolb (2003) catalog, the longest period definite SU UMa type star is TU Men, which is located in the period gap. The orbital period of OGLE-BLG-DN-002 is lightly shorter than for TV Col which shows superhumps and is classified as an intermediate polar. Vrielmann *et al.* (2004) discussed candidate intermediate polars showing superoutbursts. The outbursts of OGLE-BLG-DN-002 can be classified as superoutbursts. The one observed for OGLE-BLG-DN-003 is more difficult to be un-

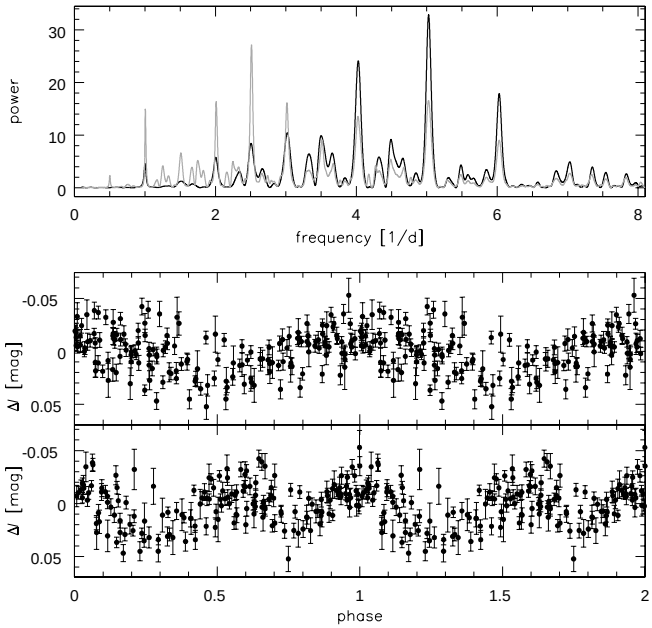

Fig. 9. Periodogram of plateau data (*upper panel*) and the light curve phased with two candidate periods: 0.19895 d (*middle panel*) and 0.39803 d (*lower panel*) for OGLE-BLG-DN-003. The periodogram is shown for one (black line) and two (gray line) harmonics.

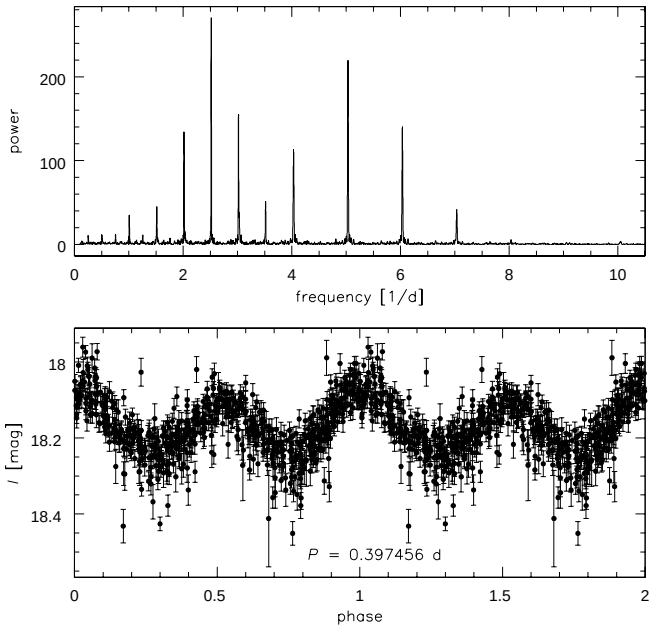

Fig. 10. Power spectrum of the quiescence data of OGLE-BLG-DN-003 from 2011 (*upper panel*) and these data phased with the period of 0.397456(41) d corresponding to the highest peak in the power spectrum (*lower panel*).

ambiguously classified. The observational characteristics of OGLE-BLG-DN-002 and OGLE-BLG-DN-003 do not allow one to convincingly classify these objects in the currently used scheme.

We have shown that the OGLE-IV photometry acquired with a 20 minute cadence can be used for investigation of DNe. In the future we plan to publish an in-depth analysis of the most interesting objects, as well as present a catalog of such objects in our Galactic bulge fields. The total area covered by the OGLE-IV survey with a cadence higher than one observation per night is larger than 70 square degrees, thus, we expect a few hundreds of DNe to be found. It is also planned to extend the OGLE real time variable stars monitoring systems (Udalski 2003) to the discovered DNe allowing real time checking of their current state (outburst, quiescence).

Acknowledgements. The OGLE project has received funding from the European Research Council under the European Community's Seventh Framework Programme (FP7/2007-2013)/ERC grant agreement No. 246678. RP is supported through the Polish Science Foundation START program. JS acknowledge support by the Space Exploration Research Fund of the Ohio State University.

REFERENCES

Alard, C., and Lupton, R.H. 1998, *ApJ*, **503**, 325.
Alard, C. 2000, *A&AS*, **144**, 363.
Cieslinski, D., Diaz, M.P., Mennickent, R.E., and Pietrzyński, G. 2003, *PASP*, **115**, 193.
Cieslinski, D., Diaz, M.P., Drake, A.J., and Cook, K.H, 2004, *PASP*, **116**, 610.
Howell, S.B., Nelson, L.A., and Rappaport, S. 2001, *ApJ*, **550**, 897.
Kato, T., Imada, A., Uemura, M. *et al.* 2009, *PASJ*, **61**, 395.
Knigge, C. 2006, *MNRAS*, **373**, 484.
Olech, A., *et al.* 2011, astro-ph/1103.5754.
Osaki, Y., Meyer, F., and Meyer-Hofmeister, E. 2001, *A&A*, **370**, 488.
Retter, A., Hellier, C., Augusteijn, T., Naylor, T., Bedding, T.R., Bembrick, C., McCormick, J., and Velthuis, F. 2003, *MNRAS*, **340**, 679.
Ritter, H., and Kolb, U. 2003, *A&A*, **404**, 301.
Sako T., *et al.* 2008, *Experimental Astronomy*, **22**, 51.
Schwarzenberg-Czerny, A. 1996, *ApJ*, **460L**, 107.
Semeniuk, I., Olech, A., Kwast, T., and Należyty, M. 1997, *Acta Astron.*, **47**, 201.
Skowron, J., Wyrzykowski, Ł., Mao, S., and Jaroszyński, M. 2009, *MNRAS*, **393**, 999.
Southworth, J., Copperwheat, C. M., Gänsicke, B.T., and Pyrzas, S. 2010, *A&A*, **510**, 100.
Stolz, B., and Schoembs, R. 1984, *A&A*, **132**, 187.
Szkody, P., *et al.* 2007, *AJ*, **134**, 185.
Tylenda, R., Hajduk, M., Kamiński, T., Udalski, A., Soszyński, I., Szymański, M.K., Kubiak, M., Pietrzyński, G., Poleski, R., Wyrzykowski, Ł., and Ulaczyk, K. 2011, *A&A*, **528**, 114.
Udalski, A. 2003, *Acta Astron.*, **53**, 291.
Udalski, A., Szymański, M.K., Soszyński, I., and Poleski, R. 2008a, *Acta Astron.*, **58**, 69.
Vrielmann, S., Ness, J.U., and Schmitt, J.H.M.M. 2004, *A&A*, **419**, 673.
Warner, B. 2003, "Cataclysmic Variable Stars", 2nd ed., Cambridge Univ. Press, Cambridge.
Woźniak, P.R. 2000, *Acta Astron.*, **50**, 421.